DOI:10.1093/jnci/djs471

ARTICLE

Effect of SMURF2 Targeting on Susceptibility to MEK Inhibitors in Melanoma

Michael P. Smith, Jennifer Ferguson, Imanol Arozarena, Robert Hayward, Richard Marais, Anna Chapman, Adam Hurlstone, Claudia Wellbrock

Manuscript received April 5, 2012; revised September 27, 2012; accepted September 30, 2012.

Correspondence to: Claudia Wellbrock, PhD, Molecular Cancer Studies, Wellcome Trust Centre for Cell Matrix Research, University of Manchester, Michael Smith Bldg, Oxford Rd, Manchester, M13 9PT, UK (e-mail: Claudia.Wellbrock@manchester.ac.uk).

Background The mitogen-activated protein–kinase pathway consisting of the kinases RAF, MEK, and ERK is central to cell proliferation and survival and is deregulated in more than 90% of melanomas. MEK inhibitors are currently trialled in the clinic, but despite efficient target inhibition, cytostatic rather than cytotoxic activity limits their efficacy.

Methods We assessed the cytotoxicity to MEK inhibitors (PD184352 and selumetinib) in melanoma cells by toluidine-blue staining, caspase 3 cleavage, and melanoma-sphere growth. Western blotting and quantitative real-time polymerase chain reaction were applied to determine SMAD-specific E3 ubiquitin protein ligase 2 (SMURF2), PAX3, and MITF expression. Human melanoma samples (n = 77) from various stages were analyzed for SMURF2 and PAX3 expression. RNA interference was performed to target SMURF2 during MEK inhibition in vivo in melanoma xenografts in mice and zebrafish. All statistical tests were two-sided.

Results Activation of transforming growth factor β (TGF-β) signalling sensitized melanoma cells to the cytotoxic effects of MEK inhibition. Melanoma cells resistant to the cytotoxic effects of MEK inhibitors counteracted TGF-β signalling through overexpression of the E3 ubiquitin ligase SMURF2, which resulted in increased expression of the transcription factors PAX3 and MITF. High MITF expression protected melanoma cells against MEK inhibitor cytotoxicity. Depleting SMURF2 reduced MITF expression and substantially lowered the threshold for MEK inhibitor–induced apoptosis. Moreover, SMURF2 depletion sensitized melanoma cells to the cytotoxic effects of selumetinib, leading to cell death at concentrations approximately 100-fold lower than the concentration required to induce cell death in SMURF2-expressing cells. Mice treated with selumetinib alone at a dosage of 10 mg/kg body weight once daily produced no response, but in combination with SMURF2 depletion, selumetinib suppressed tumor growth by 97.9% (95% confidence interval = 38.65% to 155.50%, $P = .005$).

Conclusions Targeting SMURF2 may be a novel therapeutic approach for increasing the antitumor efficacy of MEK inhibitors.

J Natl Cancer Inst 2013;105:33–46

The mitogen-activated protein (MAP)–kinase pathway, consisting of the kinases RAF, MEK, and ERK, is hyperactivated in more than 90% of melanomas, and this is mainly triggered by a mutated BRAF-kinase, which constitutively activates MEK (1,2). Currently, inhibitors of MEK are being evaluated in the clinic, but although they show some single-agent activity, the overall responses are much lower than expected (3,4). Importantly, the doses of MEK inhibitor used in reported trials effectively produce target inhibition and suppress proliferation (4,5). These observations suggest that cytostatic effects may not be sufficient to produce a major response in patients and that the majority of tumors are intrinsically refractory to cytotoxic effects of MEK inhibition.

Indeed, from studies in melanoma cell lines, it is clear that cytotoxic effects of MEK inhibitors in melanoma cells generally occur either at concentrations considerably higher than the concentrations needed to produce an antimitotic effect or after continuous long-term exposure to the drug (6–8). However, dose-limiting toxicity or a short half-life of the inhibitor prevents these conditions being satisfied in vivo (3,5). Moreover, frequently BRAF-mutant cells display high resistance to MEK inhibitor–induced apoptosis despite efficient target inhibition (9,10), which points to the activation of additional pathways in these cells that enable them to survive even at very low levels of ERK activation. Thus, in addition to recently discovered mechanisms reinstating MAP-kinase pathway activation in the presence of inhibitor (11–14), abrogation of the cytotoxic effects of MEK inhibitors brought about by parallel pathways must be considered as a possible resistance mechanism. Phosphatidylinositol-3-kinase or its upstream regulators activate such a pathway (10,15,16), and trials using phosphatidylinositol-3-kinase pathway inhibitors combined with MEK inhibitors are currently underway. However, like the MAP-kinase pathway, phosphatidylinositol-3-kinase signalling is

central to all nontumor cells, and the toxicity of these inhibitors is a limiting factor (17,18).

We, therefore, aimed to identify melanoma specific proteins that counteract MEK inhibitor–induced cytotoxic effects. Such proteins may be useful predictive markers for the sensitivity of melanoma cells to MEK inhibitors. Moreover, targeting such proteins may 1) improve the initial response to MEK inhibitors by enhancing their cytotoxic effects, thus overcoming primary resistance, and 2) prevent secondary acquired resistance that develops from the selection for primary resistant cells during drug treatment.

Materials and Methods

Cell Culture, Reagents, and Transfections

Human melanoma cell lines, derived from patients with either primary (888mel) or metastatic (A375, WM266-4, SK-Mel2, 501mel, and WM164) melanoma lesions, were grown in Dulbecco's modified Eagle medium containing 10% fetal calf serum (PAA, Yeovil, UK). A375, WM266-4, WM164, and SK-Mel2 cells were from American Type Culture Collection (LGC, Middlesex, UK), 501mel and 888mel were a gift from Steven Rosenberg (National Cancer Institute, Bethesda, MD). All cell lines are positive for the melanoma marker MITF: SK-Mel2 cells harbor an *NRAS* mutation, and the other melanoma cell lines were confirmed to harbor a *BRAF* mutation. Human dermal fibroblasts were a gift from Guillaume Jacquement (University of Manchester, Manchester, UK) and grown in Dulbecco's modified Eagle medium containing 10% fetal calf serum. Normal human melanocytes (Cascade Biologics, Invitrogen, Carlsbad, CA) were cultured in medium 154 with human melanocyte growth supplement 2 (Cascade Biologics). PD184352 was from Axon Medchem (Groningen, The Netherlands), and selumetinib (AZD6244) was from Selleck Chemicals (Newmarket, UK). Transforming growth factor β (TGF-β) was from Sigma (St Louis, MO). Cells were transfected with plasmid DNA using Attractene transfection reagent (Qiagen, Valencia, CA) and with small interfering RNAs (siRNAs) using INTERFERin siRNA-transfection reagent (Polyplus, Illkirch, France) according to the manufacturer's instructions. For the generation of A375 cells stably transfected with either the control vector pLKO or with different SMAD-specific E3 ubiquitin protein ligase 2 (SMURF2)–specific small hairpin RNAs (shRNAs), cells were transfected with the respective circular plasmids (set of 5 shRNAs, #RHS4533; Open Biosystems, Huntsville, AL) and selected for puromycin (1μg/ml) resistance. Clones S2-C4 and S2-C14 were isolated from cell populations transfected with different shRNA sequences. For the MEK inhibitor resistance colony formation assay, A375, WM266-4, and SK-Mel28 cells were transfected with circular pEF-MITF or empty vector plasmids. Cells were plated in 10-cm dishes and incubated with 1μM PD184352 for 3 weeks before being formalin fixed, stained with crystal violet, and photographed. Quantification was achieved by spectrophotometrical analysis measuring the optical density at 555 nm (OD 555) of the solubilized dye.

Immunoblotting

Melanoma cells (3×10^5) were lysed in 150-μL sodium dodecyl sulfate sample buffer (62.5 mM Tris-hydrochloride [pH 6.8 at 25°C], 2% weight/volume sodium dodecyl sulfate, 10% glycerol, 50 mM dithiothreitol, 0.01% weight/volume bromophenol blue) or lysis buffer [50 mm 4-(2-hydroxyethyl)-1-piperazineethanesulfonic acid, pH 7.5, 150 mM sodium chloride, 1.5 mM magnesium chloride, 1 mM ethylene glycol tetraacetic acid, 10% glycerol, 1% Triton X-100, 1 mM phenylmethanesulfonyl fluoride, 0.2 mM sodium orthovanadate, 10 mg/mL leupeptin, 10 mg/ml aprotinin) for 20 minutes at 4ºC and analyzed by standard immunoblotting protocols. The same amount of protein was loaded in each lane, and primary antibodies were detected by luminescence using peroxidase-coupled secondary antibodies (Jackson, Stratech, Newmarket, UK). The primary antibodies used were: phospho-ERK (mouse monoclonal MAPK-YT, 1:10,000 dilution; Sigma); ERK2 (rabbit polyclonal C-14, 1:10,000 dilution), PAX3 (goat-polyclonal N-19, 1:1000 dilution), and SMURF2 (rabbit polyclonal H-50, 1:1000 dilution) from Santa Cruz Biotechnolgy (Santa Cruz, CA); MITF (mouse monoclonal, C5, 1:500 dilution; Neomarkers, Lab Vision, Runcorn, UK); PARP (mouse monoclonal C2-10, #556362, 1:3000 dilution; BD Biosciences, Oxford, UK); and cleaved caspase 3, SMAD2, and phospho-SMAD2, SMAD3, and SMAD4 (all rabbit polyclonal, 1:1000 dilution) from Cell Signaling (Boston, MA).

Detection of Cell Death

The cellular sub-G_1 fraction was determined by fluorescence-activated cell sorting using propidium iodide staining and standard protocols. Quantification of live cells was performed by crystal violet or toluidine blue staining of formalin-fixed cells, and subsequent spectrophotometrical analysis was performed by measuring the OD 555 of the solubilized dye.

RNA Isolation and Quantitative Real-Time Polymerase Chain Reaction (qPCR) Analysis

RNA was isolated with TRIZOL reagent (Invitrogen), and selected genes were amplified by qPCR using SYBR green (Qiagen) incorporation during the amplification reaction. Primer sequences (forward; reverse) were as follows: PAX3 (AGGATGCGGCTGATGGAACTCACTG; CCAGGATGATGCGGCCGGGCCC GGG); MITF (CCGTCTCTCACTGGATTGGT; TACTTGGTGGGGTTTTCGAG); SMURF2 (GCAACAAGGCCAGGTGTATT; ACCACTTGCTGTTGCTGTTG); GAPDH (CAATGACCCC TTCATTGACC; GACAAGCTTCCCGTTCTCAG); and β-actin (GCAAGCAGGAGT ATGACGAG; CAAATAAAGCCATGCCAATC).

siRNAs and shRNAs

All siRNAs were from Thermo Scientific Dharmacon (Loughborough, UK). The sequences of the individual siRNAs were as follows: SMURF2#1 (GAUGAGAACACUCCAAUUA), SMURF2#2 (GACCAUACCUUCUGUGUUG), SMURF2#3 (CAAAGUGGAAUCAGCAUUA), SMURF2#4 (GAACAAC ACAAUUUACAGA), MITF#1 (GAACGAAGAAGAAGAUUU AUU), MITF#2 (AAAGCAGUACCUUUCUACCAC), MITF#3 (GACCUAACCUGUACAACAAUU), PAX3#1 (GAAACACCG UGCCGUCAGUUU), PAX3#2 (GAGACUGGCUCCAUAC GUCUU) and scrambled (nontargeting) control sequence (AAUAUAA UCACUAUCAGGUGC); S2-*p* was a ready-to-use SMURF2 *SMART*pool. The circular plasmids containing SMURF2-specific shRNAs were from Open Biosystems (Thermo Fisher, Loughborough,

UK). S2-sh#1 corresponds to clone TRCN0000003475, and S2-sh#2 corresponds to clone TRCN0000003477.

Melanoma Three-Dimensional Spheroid Growth

A375 melanoma cells and the corresponding SMURF2 shRNA derivatives stably expressing green fluorescent protein were resuspended in Dulbecco's modified Eagle medium containing 5% fetal calf serum and 1.5% methylcellulose (Sigma). The cell suspension was transferred into a 96-well plate (1000 cells per well), and spheres were allowed to form over a period of 48 to 72 hours. Spheres were then transferred into 0.5-mL fibrillar bovine dermal collagen (2.3 mg/mL; Nucaton, Leimuiden, The Netherlands) with one sphere per well of a 24-well plate. Once the collagen was set, Dulbecco's modified Eagle medium containing 10% fetal calf serum was added, and after approximately 16 hours, drugs were added to the medium at indicated concentrations. Dead cells were identified by staining of nonfixed cells with ethidium bromide (100 µg/mL; Sigma) for 10 minutes, followed by three washes with phosphate-buffered saline. Green fluorescent protein–expressing spheres were monitored, and ethidium bromide intensity was assessed using a Leica DM IL HC inverted microscope and a FC340 Cooled Monocrome camera (Leica Microsysytems).

Melanoma cDNA Tissue Array

Two melanoma TissueScan cDNA arrays, MERT101 and MERT102 (Origene, Rockville, MD), were analyzed for the expression of SMURF2 and PAX3. The arrays consisted of cDNA derived from stage III (n = 36) and stage IV (n = 41) melanomas, staged according to the revised TNM classification with minimum stage grouping (19), and from normal skin (n = 6), which was supplemented with additional cDNA derived from human fibroblasts, keratinocytesm, and melanocytes. The expression in melanocytes was set to one. The cDNA samples were preamplified using the TaqMan PreAmp Master Mix Kit (PN4384267, Applied Biosystems, Carlsbad, CA) according to the manufacturer's instructions. qPCR was carried out with TaqMan Gene Expression Master Mix (PN4369016, Applied Biosystems). β-Actin expression was used to normalize relative SMURF2 and PAX3 expression. Experiments were performed as multiplex PCR reactions using TaqMan probes (Applied Biosystems) for SMURF2 (Hs00224203, FAM labelled) or PAX3 (Hs00240950, FAM labelled) with a differentially labelled β-actin probe (Hs99999903, VIC labelled).

Melanoma Xenografts

All procedures involving animals were approved by the Animal Ethics Committees of the Institute of Cancer Research in accordance with National Home Office regulations under the Animals (Scientific Procedures) Act 1986 and according to the guidelines of the Committee of the National Cancer Research Institute (20).

Xenografts in Zebrafish. Zebrafish (*Danio rerio*) were raised and maintained at the University of Manchester Biological Services Unit. Zebrafish xenografts were generated by injection of approximately 1000 melanoma cells into the pericardiac space surrounding the heart of embryos that were 48 hours postfertilization. Subsequently, groups of six larvae per condition, randomly assigned were treated with either 20 nM or 100 nM PD184352 or the vehicle dimethyl sulfoxide (DMSO). The drug was added to the fish medium, and larvae were grown at 34°C ambient temperature in chorion water. Before drug addition (day 1) and 3 days after drug addition, anesthetized larvae (MS222, Sigma) were imaged using a Leica SP5 confocal microscope (Leica Microsystems). Images were processed using Volocity software (Perkin Elmer, Cambridge, UK.)

Xenografts in Mice. For xenografts, 4×10^6 A375pLKO or A375 S2-C14 cells in 0.1 mL phosphate-buffered saline were inoculated subcutaneously into one flank each of female CD1 nude mice (Charles River, Margate, Kent, UK). When mice had developed melanoma nodules of approximately 100 mm^3, mice were randomly assigned to five per group, and drug administration was initiated (day 0). Treatment was by oral gavage once daily with vehicle (5% DMSO, 95% water), or 3 mg or 10 mg/kg body weight selumetinib in vehicle. Tumor size was determined at days 7, 12, 19, 26, and 29 by calliper measurements of tumor length, width, and depth, and volume was calculated as volume = 0.5236 × length × width × depth (mm).

Statistical Analysis

All experiments were performed a minimum of three times. Data represent the results for assays performed in triplicate or more, and error bars represent 95% confidence intervals (CIs). All statistics were based on continuous variables. Comparisons between more than two treatment groups were made using predominately one-way analysis of variance with Tukeys's, Dunnett's or Bonferroni's post hoc test for multiple comparisons. For comparisons between two groups, the Student's *t* test was applied. Drug dose–response curves were analyzed with a nonlinear regression curve fit model. A ranking linear regression fit with Wald–Wolfowitz runs test was used to compare SMURF2 and PAX3 expression from cDNA array data. *P* values of less than.05 were considered statistically significant. All statistical tests were two-sided. All statistical analysis and calculations were performed using GraphPad Prism version 4.00 for Mac OS (GraphPad Software Inc, San Diego, CA).

Results

MITF Expression and Resistance to MEK Inhibitor–Induced Apoptosis in Melanoma Cells

To identify melanoma specific proteins allowing survival in the presence of MEK inhibitor, we exposed BRAF-mutant A375 melanoma cells to cytotoxic concentrations of PD184352 for 4 days and isolated individual clones that were able to grow in the presence of drug (Figure 1, A). Immunoblot analysis of individual clones for expression of the central regulator of melanoma cell fate, MITF (21–24), identified increased expression compared with the parental cell line A375 (Figure 1, B). Further analysis confirmed that in contrast with parental A375 cells, A375-R1 and A375-R4 cells were able to survive in the presence of MEK inhibitor, which was indicated by the absence of an increased subG1 fraction after MEK inhibitor exposure (Figure 1, C). However, the two resistant clones still responded to the MEK inhibitor with reduced ERK phosphorylation (Figure 1, D) and reduced progression into S-phase when compared with the parental cells (cells in S-phase: R1: 25.6% vs 7.12%, difference = 18.48%, 95% CI = 13.53 to 23.42, *P* = .002; R4: 27.87%

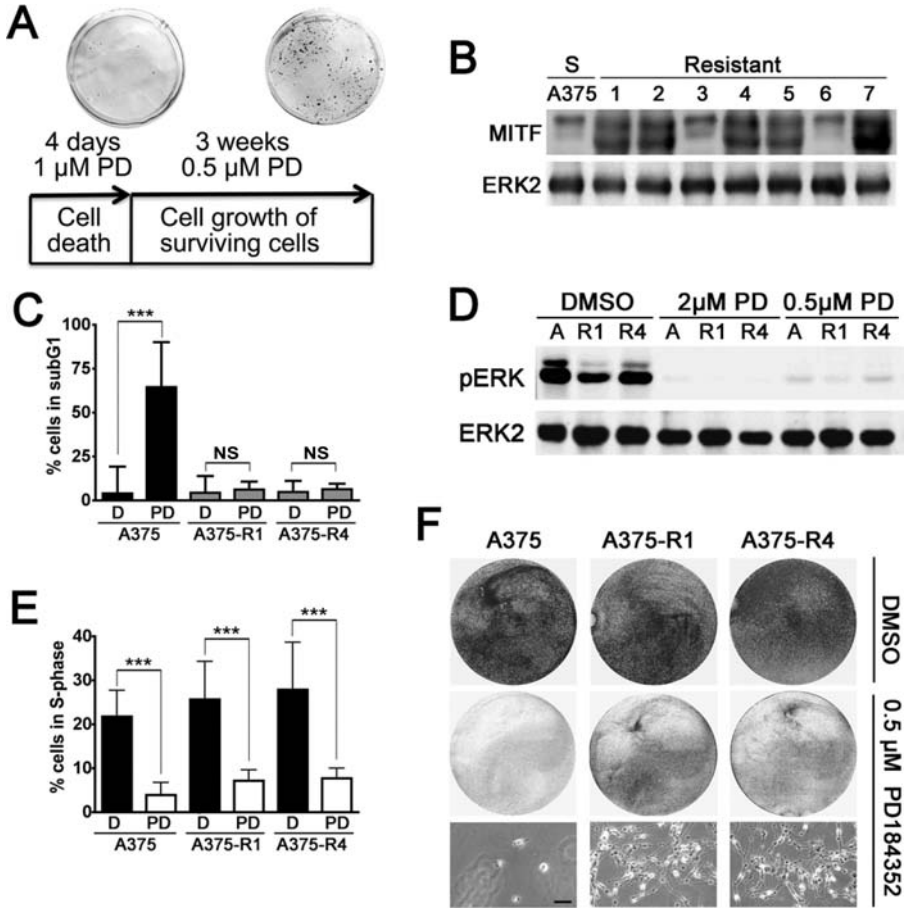

Figure 1. MITF and resistance to MEK inhibitor–induced apoptosis. **A**) Schematic of the protocol used for the selection of MEK inhibitor resistant clones. A375 melanoma cells were exposed to 1 μM PD184352 (PD) for 4 days, which resulted in greater than 98% cell death. Surviving cells were expanded at 0.5 μM PD184352 for an additional 3 weeks. Individual clones that had grown in the presence of 0.5 μM drug were isolated. **B**) Western blot of sensitive (S) parental A375 cells and MEK inhibitor–resistant clones for MITF and ERK2 (loading control). **C**) Quantification of cells in the subG1 fraction of a fluorescence-activated cell sorting (FACS) analysis of parental A375 cells and MEK inhibitor–resistant clones treated with dimethyl sulfoxide (DMSO) (D) or 1μM PD184352 (PD) for 72 hours. Bars represent means from three independent experiments; error bars refer to 95% confidence intervals; ***$P < .001$; NS = $P > .05$. A two-sided Student's *t* test was used. **D**) Western blot for phosphoERK (pERK) and ERK2 (loading control) of parental A375 cells (A) and MEK inhibitor resistant clones (R1, R4) treated with either DMSO or the indicated concentrations of PD184352 (PD). **E**) Quantification of cells in the S-phase fraction of a FACS analysis of parental A375 cells and MEK inhibitor–resistant clones treated with DMSO (D) or 1μM PD184352 (PD) for 72 hours. Bars represent means from three independent experiments; error bars refer to 95% confidence intervals; ***$P < .001$. A two-sided Student's *t* test was used. **F**) Parental A375 and resistant clones R1 and R4 were cultured in the absence (DMSO) or presence of 0.5 μM PD184352 for 12 days. Cells were fixed, photographed, and stained with crystal violet. The intensity of staining reflects the number of cells that had grown under the various conditions. Individual photographs of cells grown in the presence of PD148352 are shown. Scale bar = 50 μm.

vs 7.7%, difference 20.17%, 95% CI = 14.93 to 25.40, $P < .001$) (Figure 1, E). As a consequence, when cultured in the presence of drug, the resistant cells displayed slow but continuous growth, as was seen in a long-term growth experiment. When, after 12 days of treatment, the number of cells in a culture dish was assessed by staining with crystal violet, the staining intensity of plates containing A375-R1 or A375-R4 cells was considerably higher than in plates containing A375 cells. The difference in cell number was also visible when cells were photographed (Figure 1, F).

MITF depletion from the resistant A375-R1 and A375-R4 cells by RNA interference (RNAi) sensitized the cells to PD184352-induced caspase 3 cleavage (Figure 2, A). Furthermore, ectopic overexpression of MITF in three different sensitive cell lines increased the number of colonies growing after 3 weeks in the presence of MEK inhibitor when compared with cell lines that had been transfected with an empty vector (OD 555 of stained cells: A375: 0.046 vs 0.300, difference = –0.25, 95% CI = –0.30 to –0.21, $P < .001$; SKMEL28: OD 555 = 0.105 vs 0.335, difference = –0.23, 95% CI = –0.28 to –0.18, $P < .001$; WM2664: OD 555 = 0.033 vs 0.155, difference = 0.12, 95% CI = –0.15 to –0.10, $P < .001$) (Figure 2, B). These initial findings indicated that MITF both is required and sufficient to produce resistance to MEK inhibitor–induced cell death.

Effect of SMURF2 on MITF Expression and MEK Inhibitor Resistance

To identify the mechanism leading to increased MITF expression in the acquired resistant A375-R1 and R4 cells, we analyzed the cells for the expression of the MITF upstream regulators BRN2 and MITF and detected increased expression of only PAX3 (Figure 3, A). PAX3 is a positive transcriptional regulator of MITF (25) and its RNAi-mediated depletion in A375 and WM266-4 melanoma cells resulted in reduced MITF levels (Supplementary Figure 1, A, available online).

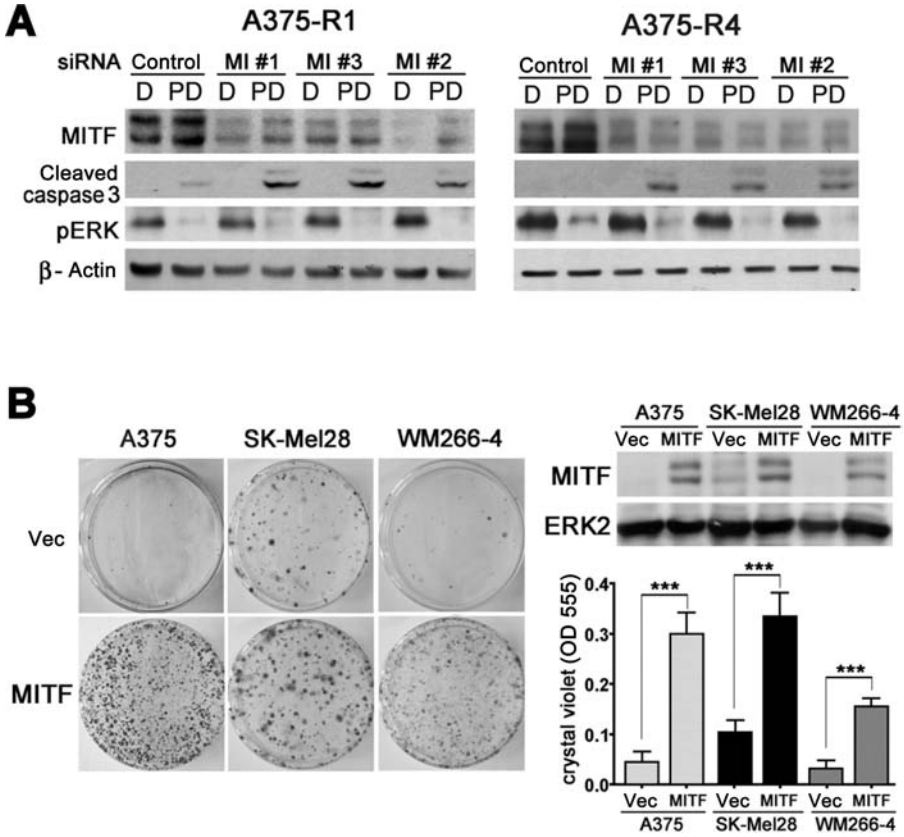

Figure 2. Effect of MITF on MEK inhibitor resistance. **A**) Western blot for MITF, cleaved caspase 3, and pERK of the resistant clones A375-R1 and A375-R4 treated with a scrambled control or MITF-specific small interfering RNAs (siRNAs) (MI #1, MI #2, MI #3) for 48 hours, followed by 24-hour exposure to 1 μM PD184352 (PD) or dimethyl sufloxide (DMSO [D]). β-Actin was used as loading control. **B**) A375, SK-Mel28, and WM266-4 cells were transfected with an MITF expression vector or an empty vector (Vec). The Western blot (upper right panels) shows MITF expression 24 hours after the transfection. Note that the chosen short-film exposure does not detect endogenous MITF expression in WM266-4 and A375 cells. The cells were cultured for 3 weeks in the presence of PD184352, and resistant colonies were stained with crystal violet. A representative stained cell image is shown to the left of the graph, which plots the mean number of crystal violet–positive cells from three independent assays; error bars refer to 95% confidence intervals; ***P < .001. A two-sided Student's t test was used.

PAX3 and MITF regulation have been placed downstream of TGF-β in melanocytes, where a SMAD4/SMAD2-containing complex directly suppresses PAX3 expression (26). We found this described mechanism was conserved in melanoma cells, where treatment of the melanoma cells with TGF-β suppressed PAX3 and MITF RNA expression when compared with nontreated melanoma cells (normal human melanocytes: relative PAX3 expression in untreated cells = 1 vs 0.43, in TGF-β-treated cells, difference = 0.57, 95% CI = 0.21 to 0.92, P < .001; relative MITF expression in untreated cells = 1 vs 0.17, in TGF-β-treated cells, difference = 0.83, 95% CI = 0.48 to 1.19, P < .001; A375: relative PAX3 expression in untreated cells = 1 vs 0.28 in TGF-β-treated cells, difference = 0.72, 95% CI = 0.36 to 1.07, P < .001; relative MITF expression in untreated cells = 1 vs 0.64 in TGF-β-treated cells, difference = 0.36, 95% CI = 0.05 to 0.72, P = 0.02) (Figure 3, B). Treatment of A375-R1 and R4 cells with TGF-β and PD184352 induced caspase 3 cleavage (Figure 3, C). Moreover, the treatment of melanoma cells with TGF-β and PD184352 reduced cell survival in the acquired resistant melanoma cells, with approximately 80% reduction in cell numbers (R1: 78.5%, 95% CI = 75.74% to 83.16%, P < .001; R4: 81.5%, 95% CI = 79.75% to 83.07%, P < .001) (Figure 3, D).

Because activating TGF-β signalling suppressed MITF expression and sensitized melanoma cells to MEK inhibitor–induced cell death, we hypothesized that counteracting TGF-β signalling could provide a mechanism for MITF-mediated MEK inhibitor resistance. Indeed, we detected statistically significantly (R1: P < .001; R4: P < .001) increased RNA expression of SMURF2 (Figure 3, E), an E3 ubiquitin ligase that regulates the degradation and activity of SMAD proteins (27,28) in the MEK inhibitor–resistant cell lines compared with the parental A375 cells. We found that SMURF2 suppresses the amount of SMAD2 in melanoma cells (Figure 3, E; Supplementary Figure 2, A, available online), and that high SMURF2 levels paralleled high PAX3 expression in A375-R1 and A375-R4 cells (Figure 3, F). This high PAX3 expression is dependent on SMURF2 because SMURF2 depletion using four individual siRNAs completely abolished increased PAX3 expression (Figure 3, F). Accordingly, MITF expression was also severely reduced (Supplementary Figure 2, C and D, available online).

Depletion of SMURF2 from A375-R1 or A375-R4 cells did not impact their viability, but additional treatment with PD184352 induced cell death (Supplementary Figure, 2, B and E, available online). A dose–response analysis showed that SMURF2 depletion via RNAi overcomes MEK inhibitor resistance, and the GI_{50} (concentration of MEK inhibitor required to reduce the cell number by 50% compared with DMSO control) for PD184352 in A375-R1 and A375-R4 cells was reduced 3- to 10-fold compared

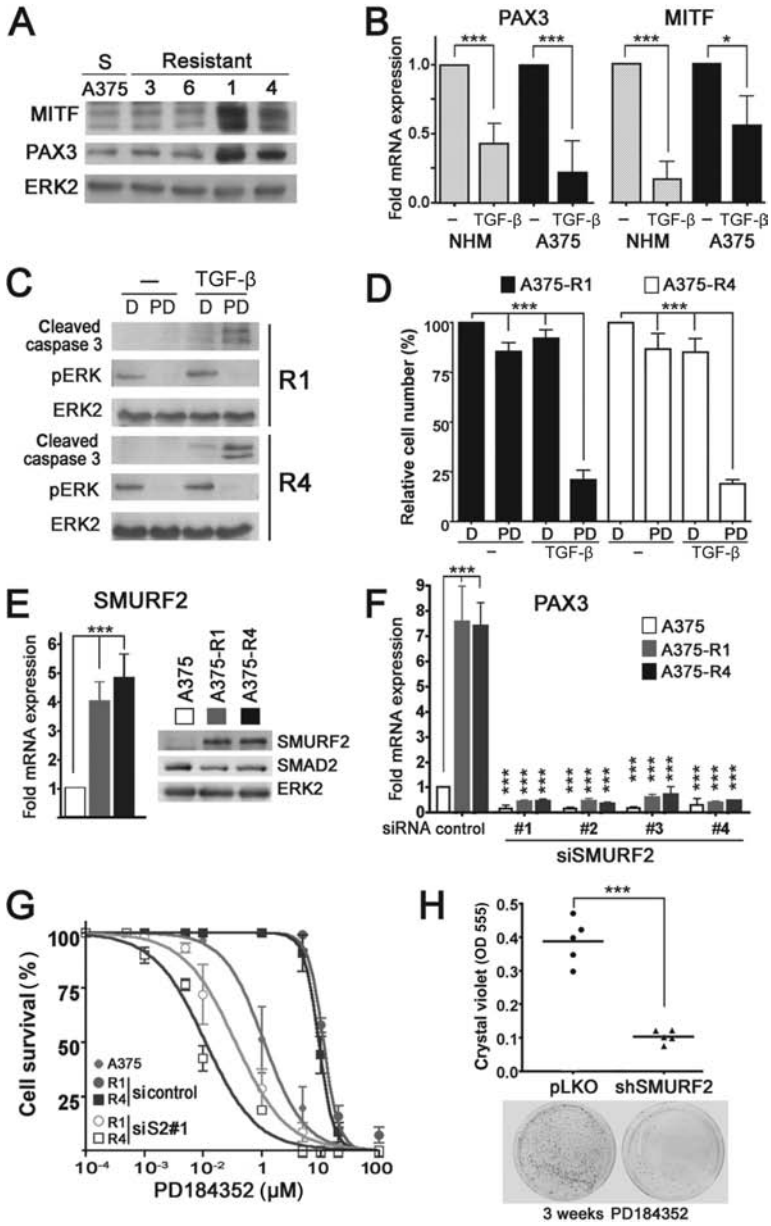

Figure 3. Effects of transforming growth factor β (TGF-β) and SMURF2 on melanoma cell sensitivity to MEK inhibition. **A**) Western blot of sensitive (S) parental A375 cells and MEK inhibitor resistant clones R3, R6, R1, and R4 for MITF, PAX3, and ERK2 (loading control). **B**) Quantitative real-time polymerase chain reaction (PCR) analysis of PAX3 and MITF expression in normal human melanocytes (NHM) and A375 cells either unstimulated (–) or stimulated (transforming growth factor β [TGF-β]) for 24 hours with 5 ng/ml TGF-β. Bars represent means from three independent experiments; error bars refer to 95% confidence intervals; ***$P < .001$; *$P = .02$. A two-sided Student's t was used. **C**) Western blot of A375-R1 and A375-R4 cells for cleaved caspase 3, pERK,and ERK2 (loading control).The cells were either unstimulated (–) or stimulated (TGF-β) for 24 hours with 5 ng/ml TGF-β in the presence of dimethyl sulfoxide (DMSO [D]) or 2 μM PD184352 (PD). **D**) Quantification of cell survival. A375-R1 and A375-R4 cells were treated with TGF-β for 48 hours, followed by 24-hour exposure to 2 μM PD184352 (PD) or DMSO (D), before the cell number was assessed by toluidine staining. DMSO-treated cells were set 100%. Bars represent means from three independent experiments; error bars refer to 95% confidence intervals; ***$P < .001$. Two-sided analysis of variance (ANOVA) with Bonferroni post hoc test was used. **E**) Quantitative real-time PCR and Western blot analysis of SMURF2 expression in parental A375 cells and the resistant clones R1 and R4. SMURF2 expression in A375 cells was set to 1. Bars represent means from three independent experiments; error bars refer to 95% confidence intervals; ***$P < .001$. A two-sided Student's t test was used. **F**) Quantitative real-time PCR analysis of PAX3 expression in parental A375 cells and the resistant clones R1 and R4 transfected with either a scrambled control or four individual SMURF2-specific small interfering RNAs (siRNAs) (#1–#4). A375 cells treated with a scrambled control siRNA were set to 1. Bars represent means from three independent experiments; error bars refer to 95% confidence intervals. ***$P < .001$. Two-sided ANOVA with Dunnett's post hoc test was used. **G**) Dose–response curve of cell survival in the presence of PD184352. A375 cells and the resistant clones R1 and R4 were treated with a scrambled control or a SMURF2-specific siRNA (siS2#1) for 48 hours, followed by the indicated concentrations of PD184352 for 24 hours before they were fixed, stained with toluidine blue, and quantified measuring the optical density at 555 nm (OD 555) of solubilized dye. For each cell line, DMSO-treated cells were set to 100%, and percentage of cell survival at defined drug concentrations was determined. Drug dose–response curves were analyzed with a nonlinear regression curve fit model. **H**) A375-pLKO or small hairpin SMURF2-expressing A375 cells (clone S2–C14; see Supplementary Figure 3, available online) were cultured for 3 weeks in the presence of 0.5 μM PD184352, and resistant colonies were stained with crystal violet, and the OD 555 was quantified. Values represent the results of five independent experiments. ***$P < .001$. A two-sided Student's t test was used. Black circles represent cells stably transfected with the empty pLKO vector, black triangles represent cells stably transfected with a SMURF2–small hairpin RNA–expressing vector.

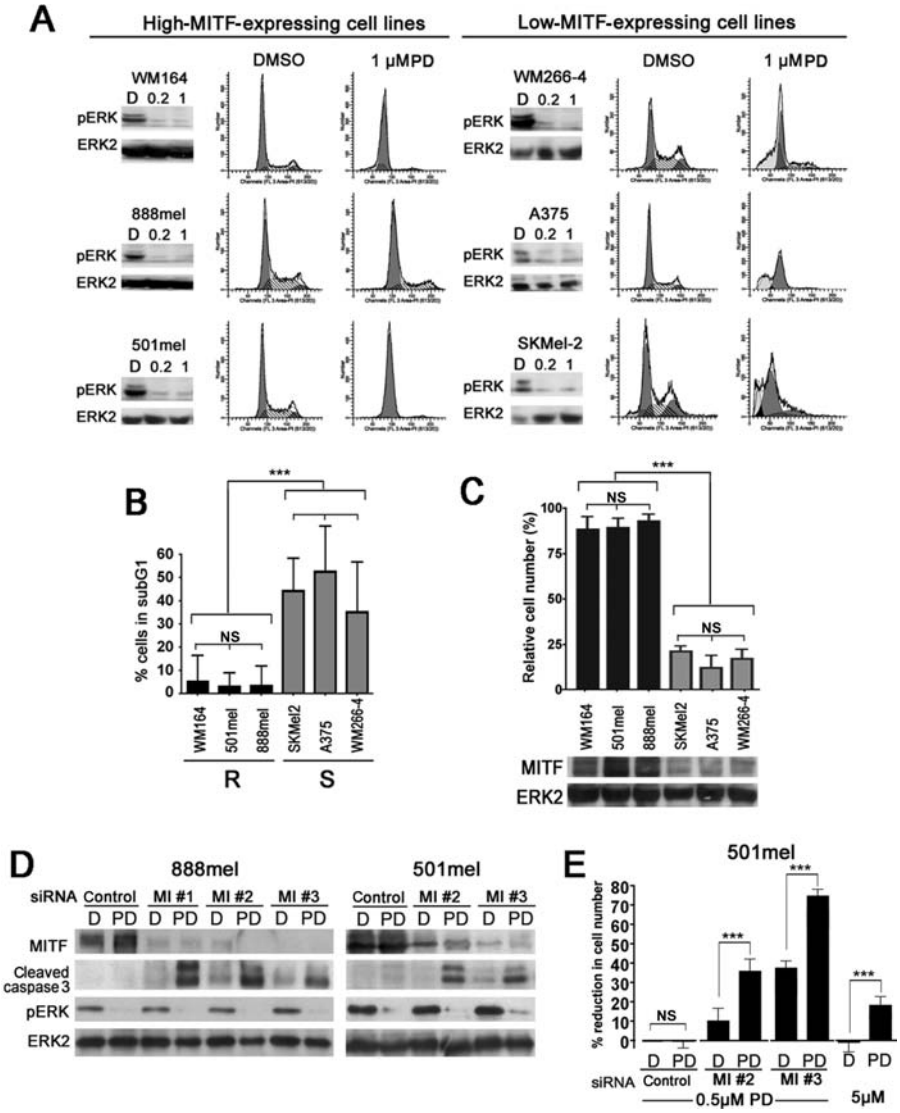

Figure 4. MITF and primary resistance to MEK inhibition. **A**) DNA content fluorescence-activated cell sorting (FACS) analysis (assessing fractions of cells in G1, S, G2/M, or subG1 phase) of the indicated cell lines treated with 1μM PD184352 (PD) or dimethyl sulfoxide (DMSO) for 72 hours. Western blots of ERK phosphorylation (pERK) at concentrations of 0.2 and 1 μM PD184352. ERK2 serves as loading control. **B**) Quantification of cells in the subG1 fraction of a FACS analysis of the indicated melanoma cell lines (R = resistant, S = sensitive) treated with 1μM PD184352 for 72 hours. Bars represent means from three independent experiments; error bars refer to 95% confidence intervals. NS = $P > .05$; ***$P < .001$. Two-sided analysis of variance (ANOVA) with Tukey's post hoc test was used. **C**) Quantification of toluidine staining of live cells of the indicated melanoma cell lines treated with 3 μM PD184352 for 24 hours or DMSO only. DMSO-treated cells were set to 100%. Bars represent means from three independent experiments; error bars refer to 95% confidence intervals. NS = $P > .05$; ***$P < .001$. Two-sided ANOVA with Tukey's post hoc test was used. A Western blot showing MITF expression and ERK2 as loading control is shown. **D**) Western blot of MITF, cleaved caspase 3, and phospho-ERK (pERK) for 888mel and 501mel cells treated with a scrambled control or MITF-specific small interfering RNAs (siRNAs) (MI#1–#3) for 48 hours, followed by 24-hour exposure to 1 μM PD184352 (PD) or DMSO (D). ERK2 was used as loading control. **E**) Quantification of cell survival. 501mel cells were treated with a scrambled control or MITF-specific siRNAs (MI#2 and #3) for 48 hours, followed by 24-hour exposure to 0.5 μM PD184352 (PD) or DMSO (D). They were then fixed and stained with toluidine blue, and the optical density at 555 nm was quantified. DMSO-treated cells were set to 100%, and treatment with 5 μM PD184352 was used as positive control. Bars represent means from three independent experiments; error bars refer to 95% confidence intervals; NS = $P > .05$; ***$P < .001$. Two-sided ANOVA with Tukey's post hoc test was used.

with A375 cells (A375: 95% CI [GI_{50}] = 1.47 to 2.66 μM; R1/siS2: 95% CI [GI_{50}] = 0.53 to 0.72 μM; R4/siS2: 95% CI [GI_{50}] = 0.11 to 0.18 μM) (Figure 3, G). Most important, stable expression of a SMURF2-specific shRNA in A375 cells (Supplementary Figure 3, available online) suppressed the development of acquired MEK inhibitor resistance, and the number of PD184352-resistant colonies derived from small hairpin SMURF2 (shSMURF2) cells after 3 weeks of drug exposure was severely reduced when compared with empty vector pLKO cells treated with MEK inhibitor (OD 555 of stained cells, pLKO vs shSMURF: 0.3872 vs 0.1030, difference = 0.28, 95% CI = 0.21 to 0.36, $P < .001$) (Figure 3, H).

MITF Expression and Primary Resistance to MEK Inhibitor–Induced Cytotoxicity

We next extended our study to primary (innate) resistance to MEK inhibition in BRAF-mutant melanoma cells. High-MITF-expressing cells (WM164, 888mel, 501mel), which are representative of certain cohorts of melanomas (29), responded to

PD184352 with MEK inhibition even at low doses of inhibitor (0.2 μM), detectable by reduced ERK phosphorylation (Figure 4, A). However, whereas PD184352 induced a cytostatic effect in high-MITF-expressing cells, it produced cell death in low-MITF-expressing cell lines (WM266-4, A375, SKMel-2), which was seen in an increased subG1 fraction and decreased cell numbers in SKMel-2, A375 and WM266-4 cells (Figure 4, A–C).

As seen with the acquired resistant cells, depletion of MITF from high-MITF- expressing primary resistant cell lines (888mel and 501mel cells) resulted in sensitization to PD184352, which led to the activation of an apoptotic program through caspase 3 cleavage (Figure 4, D) and reduced cell numbers at low concentrations of drug (Figure 4, E).

SMURF2 Depletion and MEK Inhibitor–Induced Cytotoxicity

When we analyzed primary MEK inhibitor–resistant melanoma cells for PAX3, we found increased expression in the resistant cell lines, which paralleled increased MITF expression (Figure 5, A). Furthermore, in line with PAX3 acting upstream of MITF, PAX3 depletion from A375 cells enhanced the proapoptotic effect of PD184352 detectable by increased caspase 3 cleavage (Supplementary Figure 1, B, available online). In addition, PAX3 depletion further reduced the number of living cells in the presence of PD184352 (A375 control siRNA transfected, PD184352 treated vs A375 PAX3 siRNA transfected, PD184352 treated: 75.12% vs 44.93%, difference = 30.19%, 95% CI = 27.50% to 41.80%, P < .001) (Figure 5, B). However, ectopic expression of MITF rescued A375 cells in which PAX3 was targeted by RNAi and MEK by PD184352 (A375 PAX3 siRNA transfected, PD184352 treated vs MITF-A375 PAX3 siRNA transfected and PD184352 treated: 44.93% vs 85.07%, difference = 40.15%, 95% CI = 45.69% to 34.60%, P < .001) (Figure 5, B). On the other hand, when MITF was depleted by RNAi in ectopic MITF-expressing A375 cells, they became responsive to PD184352, and the cell number was reduced (Figure 5, B).

TGF-β induced caspase 3 cleavage in response to the presence of PD184352 (Figure 5, C). Importantly, this caspase 3 cleavage in response to TGF-β was seen not only in MEK inhibitor–sensitive WM266-4 cells but also in MEK inhibitor–resistant 501mel cells (Figure 5, C). The action of TGF-β and PD184352 was also reflected in effects on cell survival, most notably in MEK inhibitor–resistant melanoma cells (Figure 5, D).

When we analyzed our panel of melanoma cells, we found statistically significantly (P = .001) increased SMURF2 expression in the primary MEK inhibitor–resistant cell lines compared with the MEK inhibitor–sensitive cell lines. (Figure 5, E). When SMURF2 was depleted by RNAi in melanoma cell lines, this resulted in reduced PAX3 and MITF expression (Supplementary Figures 2 and 3, available online), and because reduced PAX3 and MITF expression sensitizes melanoma cells to MEK inhibition (Figure 1, Figure 2, A, Figure 5, B), SMURF2 depletion strongly increased cell death in melanoma cells in the presence of PD184352 (A375,scrambled control siRNA transfected, PD184352 treated vs A375, S2 siRNA transfected PD184352 treated: 79.58% vs 13.47%, difference = 66.11%, 95% CI = 57.27% to 74.94%, P < .001) (Figure 5, F). However, ectopic expression of MITF, which is not affected by SMURF2 depletion (Supplementary Figure 1, C, available online), rescued the MEK inhibitor effect on the cell number (A375, S2 siRNA transfected PD184352 treated vs MITF-A375, S2 siRNA transfected PD184352 treated: 13.47% vs 81.18%, difference = 67.71%, 95% CI = 73.95% to 61.47%, P < .001) (Figure 5, F). This suggests that reduced MITF expression is responsible for the cell death induced by SMURF2 depletion in PD184352-treated cells.

SMURF2 Expression in Melanoma and Effect of Its Depletion in Melanoma Cells

In our panel of melanoma cell lines, SMURF2 depletion had no major effect on cell viability (Figure 6, A). However, compared with single treatments, combined targeting of SMURF2 and MEK produced statistically significant (P < .001) cell death, most notably in the primary resistant cell lines (Figure 6, A). On the other hand, SMURF2 depletion had no noticeable effect on melanocytes (Figure 6, B). We also did not observe any major effect on cell survival when SMURF2 was depleted and MEK inhibited in non-MITF-expressing but BRAF-mutant colon cancer cells (Figure 6, C), supporting a melanoma-specific role for SMURF2. When melanoma cells were grown as spheres in three-dimensional collagen, SMURF2 depletion enhanced PD184352-induced cell death, visible by ethidium bromide uptake (Figure 6, D). Furthermore, targeting SMURF2 in fibroblasts did not stimulate tumor-promoting effects otherwise produced by TGF-β (30), such as increased expression of VEGF and SPARC (Figure 6, E), which reveals an important difference between SMURF2 function and TGF-β stimulated signalling.

In advanced stage III and IV melanomas, SMURF2 RNA expression was statistically significantly increased compared with normal skin (mean of different skin samples and primary skin cells [normal melanocytes = 1] 1.05-fold vs stage III 15.40-fold, difference = 14.35, 95% CI = 21.91-fold to 6.80-fold, P < .001; normal 1.05-fold vs stage IV 8.01-fold, difference = 6.96, 95% CI = 10.69-fold to 3.25-fold, P < .001) (Figure 6, F). There was a correlation (r^2 = 0.788) between SMURF2 and PAX3 expression (Figure 6, G), suggesting that the regulatory link between these two proteins is preserved in the tumors.

Effect of SMURF2 Depletion on MEK Inhibition In Vivo

In an approach that allows rapid assessment of cytotoxic effects in an in vivo setting, MEK inhibitor–resistant 501mel or MEK inhibitor–sensitive A375 cells were injected into zebrafish embryos (Figure 7, A; Supplementary Figure 4, available online). Both, pLKO-control and SMURF2-depleted cells (ie, cells stably expressing SMURF2-specific shRNAs; see also Figure 3, H) grew with no statistically significant difference (P > .05) in size over 3 days (Figure 7, A; Supplementary Figure 4, B, available online). Xenografts formed by sensitive A375 cells showed no statistically significant tumor growth over a period of 3 days (day 1 to day 4) at 20nM PD184352 (P > .05) (Supplementary Figure 4, B, available online). Resistant 501mel xenografts grew even in the presence of 100 nM drug (Figure 7, A), but additional SMURF2 depletion reduced the xenograft volume to less than 0.5-fold of the initial size measured at day 1 (DMSO: pLKO 3.26-fold vs shSMURF2 2.78-fold size increase compared with day 1, difference = –0.48,

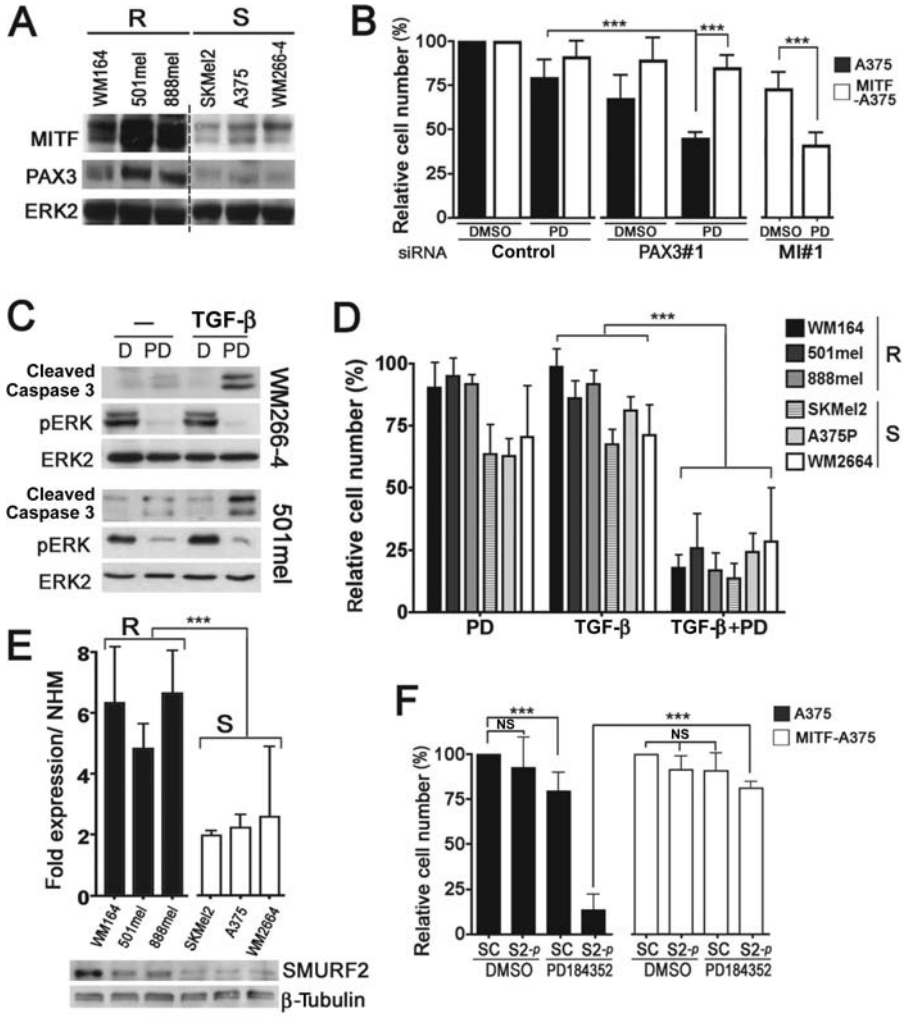

Figure 5. SMURF2 confers resistance to MEK inhibition in melanoma cells. **A**) Western blot of the indicated cell lines for MITF, PAX3, and ERK2 (loading control). R = resistant, S = sensitive. **B**) Quantification of cell survival. A375 and MITF-A375 cells (stably expressing MITF from an ectopic promoter) were treated with a scrambled control, PAX3- (PAX3#1) or MITF (MI#1)-specific small interfering RNAs (siRNAs), for 48 hours, followed by 24-hour treatment with 1 μM PD184352 or dimethyl sulfoxide (DMSO). They were then stained with toluidine blue, and the optical density at 555 nm was quantified. DMSO-treated cells were set to 100%. Bars represent means from three independent experiments; error bars refer to 95% confidence intervals; ***P < .001. Two-sided analysis of variance (ANOVA) with Tukey's post hoc test was used. **C**) Western blot of WM266-4 and 501mel cells for cleaved caspase 3, pERK, and ERK2 (loading control). The cells were either unstimulated (–) or stimulated (transforming growth factor β [TGF–β]) for 24 hours with 5 ng/ml TGF-β in the presence of DMSO (D) or 1 μM PD184352 (PD). **D**) Quantification of cell survival. The indicated cell lines were treated with TGF-β for 48 hours, followed by 24-hour exposure to 1 μM PD184352 (PD) or DMSO (D). They were then stained with toluidine blue, and the optical density at 555 nm was quantified. DMSO-treated cells were set to 100%. Bars represent means from three independent experiments; error bars refer to 95% confidence intervals; ***P < .001. Two-sided ANOVA with Tukey's post hoc test was used. **E**) Quantitative real-time polymerase chain reaction and Western blot analysis of SMURF2 expression in melanoma cell lines. The expression of SMURF2 is shown as fold expression compared with normal human melanocytes (NHM), in which SMURF2 expression was set to 1. Bars represent means from three independent experiments; error bars refer to 95% confidence intervals; ***P < .001. Two-sided ANOVA with Dunnett's post hoc test was used. **F**) Quantification of cell survival. A375 and MITF-A375 cells were treated with a scrambled control (SC) or SMURF2 pooled siRNAs (S2-*p*) for 48 hours, followed by 24-hour exposure to 1 μM PD184352 or DMSO, and quantified using toluidine blue. DMSO-treated cells were set to 100%. Bars represent means from three independent experiments; error bars refer to 95% confidence intervals; NS = P > .05; ***P < .001. A two-sided Student's *t* test was used.

95% CI = –0.22 to 1.19, P > 0.05; PD184352: PLKO 1.90-fold vs shSMURF2 0.57-fold size increase compared with day 1, difference = –1.33, 95% CI = –0.64 to –2.05, P < .001) (Figure 7, A). A similar effect was observed for A375 xenografts (Supplementary Figure 4, B, available online).

SMURF2 depletion led to an approximately 100-fold enhanced sensitivity of melanoma cells to selumetinib, a MEK inhibitor that produces limited responses in melanoma patients (3) (A375: (GI_{50}) = 2.2 μM, 95% CI = 2.114 to 2.286; pLKO: (GI_{50}) = 1.69 μM, 95% CI = 1.60 to 1.81 μM; S2C4: (GI_{50}) = 26.62 nM, 95% CI = 20.42 to 36.73 nM; S2C14 (GI_{50}): 23.3 nM, 95% CI = 17.24 to 31.60) (Figure 7, B). In mice, selumetinib reduces xenograft growth at doses of 25 to 30 mg/kg twice daily (9,31). However pharmacokinetic analyses revealed that a dose of 10 mg/kg once per day produces drug exposures in mice similar to those achieved in clinical use (32). Therefore, we used doses of 3 and 10 mg/kg once daily, which did not have a statistically significant effect (P > .05) on the growth of parental A375-pLKO tumors (Figure 7,

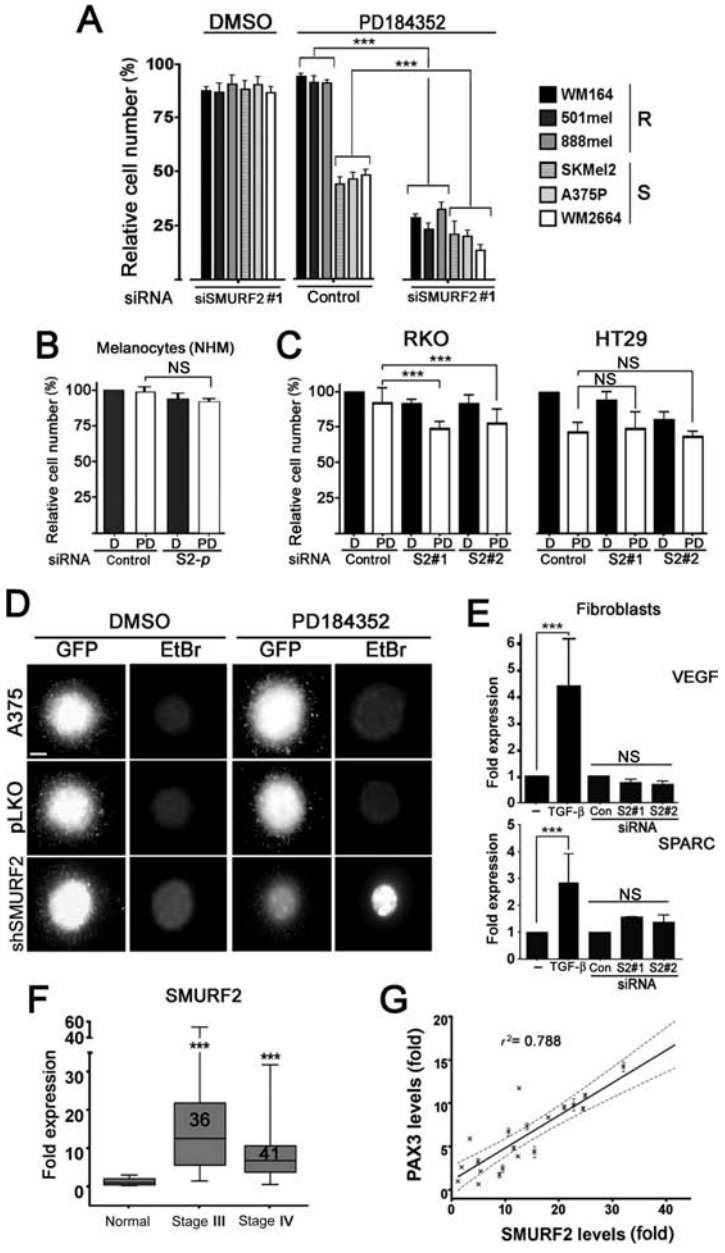

Figure 6. SMURF2 overexpression and specificity in targeting SMURF2 in melanoma cells. **A**) Quantification of cell survival. The indicated cell lines were treated with scrambled control or SMURF2-specific small interfering RNAs (siRNAs) (siSMURF2#1) for 48 hours, followed by 24-hour exposure to dimethyl sulfoxide (DMSO) or 1 μM PD184352. They were then they were stained with toluidine blue, and the optical density at 555 nm was quantified. DMSO-treated cells were set to 100%. Bars represent means from three independent experiments; error bars refer to 95% confidence intervals; ***P < .001. Two-sided analysis of variance (ANOVA) with Tukey's post hoc test was used. **B**) Quantification of cell survival. Normal melanocytes (NHM) were treated with a scrambled control or a SMURF2 pool of 4 (S2-*p*) siRNAs for 48 hours, followed by 24-hour exposure to 1 μM PD184352 (PD) or DMSO (D). They were then then fixed and stained with toluidine blue and quantified. DMSO-treated cells were set to 100%. Bars represent means from three independent experiments; error bars refer to 95% confidence intervals; NS = P > .05. A two-sided Student's t test was used. **C**) Quantification of cell survival. The colon cancer cell lines RKO and HT29 were treated with a scrambled control or two SMURF2-specific siRNAs (#1 and #2) for 48 hours, followed by 24-hour exposure to 1 μM PD184352 or DMSO. They were then fixed and stained with toluidine blue and quantified. DMSO-treated cells were set to 100%. Bars represent means from three independent experiments; error bars refer to 95% confidence intervals; NS = P > .05; ***P < .001. A two-sided Student's t test was used. **D**) Spheres of green fluorescent protein–expressing A375 cells, A375-pLKO-expressing A375 cells, or small hairpin SMURF 2(shSMURF2)–expressing A375 cells (clone S2–C14) in three-dimensional collagen were treated with DMSO or PD184352 for 3 days. Nonfixed spheres were stained with ethidium bromide (EtBr), and images were taken. Scale bar = 200 μm. **E**) Quantitative real-time polymerase chain reaction (PCR) analysis of VEGF and SPARC expression in primary fibroblasts either untreated (–) or treated (transforming growth factor [TGF-β]) with 5 ng/ml TGF-β or transfected with either a scrambled control or individual SMURF2-specific siRNAs (S2#1 and #2). Bars represent means from five independent experiments; error bars refer to 95% confidence intervals; NS = P > .05; ***P < .001. A two-sided Dunnett's t test was used. **F**) Quantitative real-time PCR analysis of SMURF2 expression in normal skin cells and stage III (n = 36) and stage IV (n = 41) melanomas. The expression was normalized to β-actin. Box plots with mean values for SMURF2 expression are shown. Normal = normal skin (n = 6), supplemented with additional cDNA derived from human fibroblasts, keratinocytes, and melanocytes. The expression in melanocytes was set to 1. ***P < .001. A two-sided Student's t test to compare expression in stage III and stage IV melanomas with normal was used. **G**) Linear regression analysis of relative SMURF2 and PAX3 expression levels in stage III melanomas. Goodness of Fit: r^2 + 0.7883. A ranking linear regression fit with Wald–Wolfowitz runs test was used to compare SMURF2 and PAX3 expression from cDNA array data.

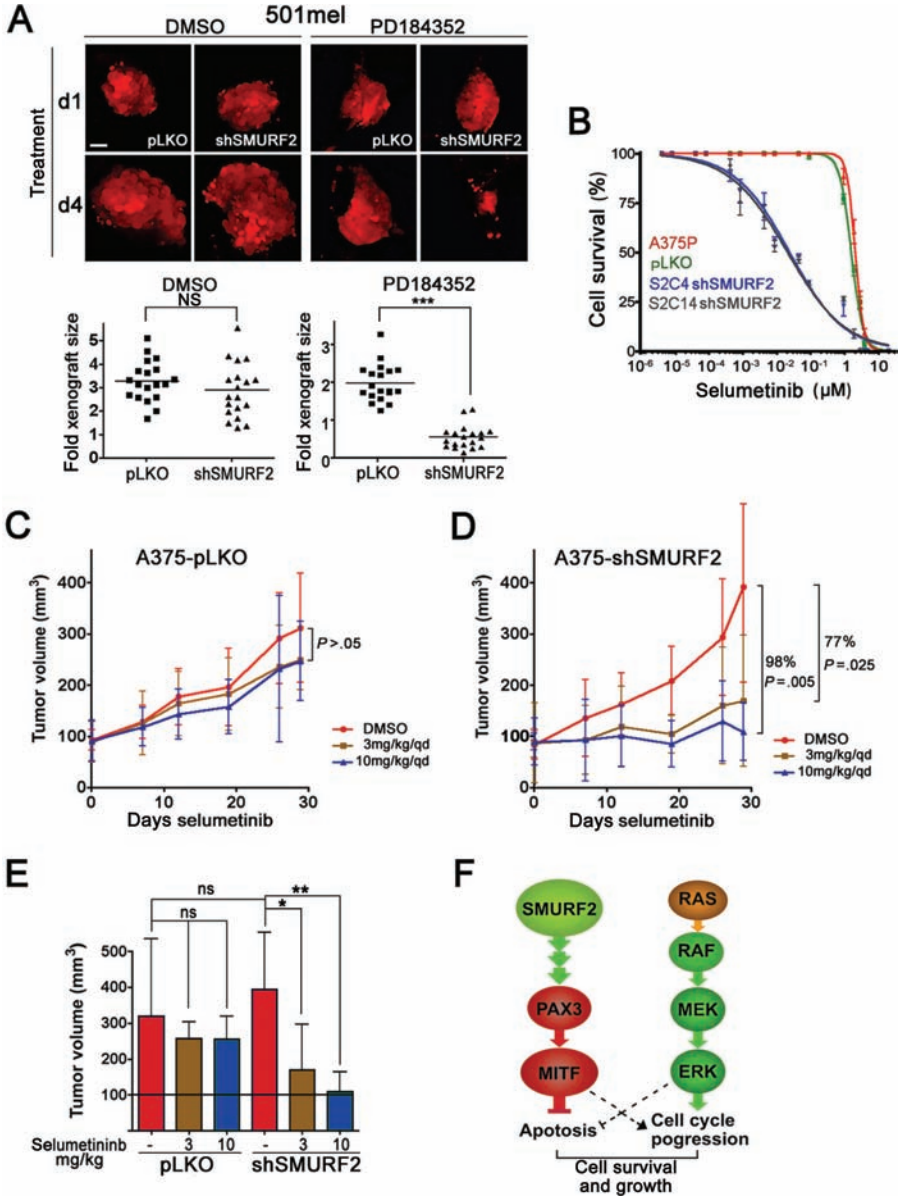

Figure 7. SMURF2 depletion sensitizes melanoma cells to MEK inhibition in vivo. **A**) RFP-expressing 501mel pLKO or small hairpin SMURF2 (shSMURF2) cells were injected into zebrafish larvae that were 48 hours post-fertilization, and the larvae were treated with either 100 nM PD184352 or the vehicle dimethyl sulfoxide (DMSO). Three days after drug addition, the xenografts were imaged. Scale bar = 36 μm. Quantification of xenograft volumes (n = 19) was performed before drug addition on day 1 and on day 4 using Volocity software. Fold xenograft size indicates the change in volume between day 1 and day 4. Black squares represent individual fish injected with pLKO-501mel cells; black triangles represent individual fish injected with 501mel-shSMURF2 cells. The horizontal bar indicates the mean value of the fold xenograft size in the respective group of zebrafish. A two-sided Student's *t* test was used to calculate *P* values; NS = $P > .05$; ***$P < .001$. **B**) Dose–response curve of cell survival in the presence of selumetinib. The indicated cell lines were treated with the indicated concentrations of selumetinib for 24 hours before they were fixed, stained with toluidine blue, and quantified. DMSO-treated cells were set to 100%, and drug dose–response curves were analyzed with a nonlinear regression curve fit model. **C**) Nude mice bearing tumors from A375-pLKO cells (empty vector) were treated with either vehicle (DMSO) or selumetininb (3 or 10 mg/kg once daily) for 29 consecutive days. The results show mean volumes measured on days 7, 12, 19, 26, and 29 for groups of five mice with error bars to represent the 95% confidence intervals. A two-sided Student's *t* test was used to calculate *P* values for day 29. **D**) Nude mice bearing tumors from SMURF2-depleted A375-S2-C14 cells were treated with either vehicle (DMSO) or selumetininb (3 or 10 mg/kg once daily) for 29 consecutive days. The results show mean volumes measured on days 7, 12, 19, 26, and 29 for groups of five mice with error bars to represent the 95% confidence intervals. A two-sided Student's *t* test was used to calculate *P* values for day 29. **E**) Quantification of tumor volume at day 29. Results shown represent a single experiment in which five mice per group were treated. Bars represent means from each group of mice; error bars refer to 95% confidence intervals; **$P = .003$; *$P = .03$; NS = $P > .05$. A two-sided Student's *t* test was used. The horizontal line at 100 mm^3 indicates the mean tumor volume at the beginning of drug treatment. **F**) Model of survival and growth regulation in melanoma cells. The cooperation of MEK and MITF is required for efficient survival. MEK predominantly regulates cell cycle progression through ERK but also activates survival signals. MITF contributes to the regulation of cell cycle progression and is required to suppress apoptosis. SMURF2 depletion on its own reduced cell cycle progression, which is entirely in line with decreased MITF expression (37). Under these conditions, MITF levels appear to be sufficient to provide survival signals as long as MEK is fully active.

C and E). However, growth of tumors derived from SMURF2-depleted A375 cells was greatly reduced at both dosing regimens, with 10 mg/kg selumetinib almost completely suppressing tumor growth and 3 mg/kg resulting in approximately 77% reduction in tumor size compared with tumors in control mice treated with the vehicle DMSO (shSMURF2/3mg/kg: difference = 77.15%, 95% CI = 10.62% to 143.72%, P = .03; shSMURF2/10mg/kg: difference = 97.9%, 95% CI = 38.65% to 155.50%, P = .005) (Figure 7, D and E).

Discussion

The efficacy of most anticancer drugs is closely linked to their cytotoxic potential. Cytostatic drugs can only stop tumor growth, which increases the risk for the development of acquired resistance because it allows for the survival and selection of cells that are able to continue to proliferate in the presence of the drug. Therefore, enhancing the cytotoxic potential of a drug will not only improve the tumor response, but it will also reduce the emergence of acquired resistance. We found that increased expression of MITF, PAX3, and SMURF2 allows melanoma cells to escape the proapoptotic effects of MEK inhibition. We identified SMURF2 as a regulator of PAX3 expression and, consequently, MITF expression and demonstrate that exploiting this mechanism dramatically enhances the cytotoxic potential of the MEK inhibitors PD184352 (CI-1040) and selumetinib (AZD6244) in vitro and in vivo.

In principle, MEK inhibitors can exert cytotoxic effects by directly activating the apoptotic programme (6–8,33). However, for this to occur, high drug concentrations and long-term drug exposure are required, suggesting that MEK's contribution to the regulation of apoptosis is not major. Rather, it appears that the predominant function of MEK is to regulate cell cycle progression through ERK, which is in agreement with observations that loss of ERK phosphorylation leads to a G1 arrest, but not always to the induction of apoptosis (7,10). In line with these findings, we identified cells that responded to the MEK inhibitor PD184352 with target inhibition and reduced proliferation but were still able to propagate in the long term, a situation likely to be found in a tumor. We found that these cells are resistant to the proapoptotic effects of MEK inhibition and that, although ERK activity is very low, it is still sufficient to promote cell cycle progression. This finding is of great relevance because it highlights the challenge of targeting the MAP-kinase pathway as a single-agent treatment. It is, therefore, of great importance to identify factors that will predict and moreover enhance the sensitivity to MEK inhibitors.

We identified the melanocyte-specific transcription factor MITF as a predictive marker for the sensitivity of melanoma cells toward the cytotoxic effect of MEK inhibitors. We found that high MITF expression protects cells from MEK inhibitor–induced cell death, which is striking considering that *MITF* is amplified in up to 20% of melanomas (34). MITF is a central regulator of melanoma cell fate because it controls differentiation, proliferation, and invasion (21,22,24). Although we do not know the exact mechanism as to how MITF regulates survival in cells in which MEK is inhibited, MITF is a known regulator of melanoma cell survival, where it can induce the expression of BCL-2 or ML-inhibitor of apoptosis and protect cells from cytotoxic agents (34–36).

We have shown previously that MITF contributes to cell cycle progression downstream of BRAF (37), but now we show that it also cooperates with MEK to provide survival signals (Figure 7, F). Although MEK can activate survival signals through ERK (7,8), it is the cooperation of both MEK and MITF that is required for survival. In this context, we identified SMURF2 as a regulator of MITF expression through PAX3 (Figure 7, F). SMURF2 depletion alone reduced cell cycle progression (Supplementary Figure 2, B, available online), which is entirely in line with decreased MITF expression. However MITF levels appear to be still sufficient to provide survival signals as long as MEK is fully active because we observed no effects on cell viability with SMURF2 depletion alone. Thus, SMURF2 itself seems to be only relevant for melanoma cells when MEK is inhibited. Importantly, we also found that depleting SMURF2 from melanocytes did not have any effect on their growth and survival. This suggests that targeting SMURF2 in normal cells does not affect viability or growth probably because of compensatory mechanisms, an assumption that is further supported by the fact that SMURF2$^{-/-}$ mice are viable and develop healthy and normal to adulthood (28). These mice eventually develop tumors; however, this occurs with a very long latency at an age of more than 20 months (38,39), suggesting that loss of SMURF2 function does not produce any immediate adverse effects.

SMURF2 is a HECT-domain E3 ubiquitin ligase, which regulates the turnover of inhibitory SMADs and associated TGF-β receptors as well as regulatory SMADs (27). SMURF2 also regulates cell polarity, motility, and senescence in a SMAD- independent manner (40–43). These findings suggest that SMURF2 plays an important role in various aspects relevant for tumor initiation and progression in a SMAD-dependent as well as SMAD-independent manner. We found that SMURF2 regulates SMAD2 levels in melanoma cells (Figure 3, E; Supplementary Figure 2, available online). However, although SMAD2 has been shown to regulate the suppression of PAX3 in melanocytes (26), the complete mechanism as to how SMURF2 suppresses PAX3 is not clear and might involve additional factors other than SMAD2. We and others detected high expression levels of SMURF2 in tumors compared with normal tissue (42,44), suggesting a deregulation of this ubiquitin ligase in cancer. On the other hand, the neutralization of SMURF2 activity by the ubiquitin-specific peptidase USP15 is important for TGF-β-mediated glioblastoma progression (45), suggesting tumor-specific differences in SMURF2 function. A tumor-specific function is supported by our finding that SMURF2 depletion from colon cancer cells did not prime these cells for MEK inhibitor cytotoxicity despite a mutant BRAF status.

We have identified SMURF2 as a potential therapeutic target in melanoma. However, there are clear limitations to our study. First we used xenograft assays to assess combined therapy in vivo, and this approach does not consider the heterogeneity found in a real tumor situation. Second, no SMURF2 inhibitor is available, and we had to rely on knock-down experiments in our study, which might produce different effects than inhibition of SMURF2 activity. Finally, we have no clinical data showing that increased expression of SMURF2 or MITF correlates with MEK inhibitor resistance, but we hope to be able to collect such samples in the future and analyze them for these potential resistance regulators.

Recent experiences with targeting kinases in patients have exposed the inevitable risk of developing resistance because of complex kinase networks and feedback mechanisms (10,13–16,46,47). Therefore, targeting a nonkinase might provide an advantage. E3 ubiquitin ligases gained a lot of attention as potential drug targets when the MDM2/p53 inhibitors Nutlin1–3 were discovered, but initial efforts to identify other E3 ubiquitin ligase inhibitors proved difficult (48). On the other hand, recent successes with inhibitors of apoptosis are encouraging (48), suggesting that developing a SMURF2-specific inhibitor might be possible. Alternatively, further characterization of the SMURF2, PAX3, and MITF regulation in melanoma may lead to the identification of better druggable proteins that can be targeted in MEK inhibitor combination therapies. Our results strongly suggest that in melanoma such therapies might have the potential to increase the frequency of complete responses and reduce the risk of the development of acquired resistance.

References

1. Davies H, Bignell GR, Cox C, et al. Mutations of the BRAF gene in human cancer. *Nature*. 2002;417(6892):949–954.
2. Wellbrock C, Hurlstone A. BRAF as therapeutic target in melanoma. *Biochem Pharmacol*. 2010;80(5):561–567.
3. Kirkwood JM, Bastholt L, Robert C, et al. Phase II, open-label, randomized trial of the MEK1/2 inhibitor selumetinib as monotherapy versus temozolomide in patients with advanced melanoma. *Clin Cancer Res*. 2012;18(2):555–567.
4. Infante JR, Fecher LA, Nallapareddy S, et al. Safety and efficacy results from the first-in-human study of the oral MEK 1/2 inhibitor GSK1120212. *J Clin Oncol*. 2010;28:15(Suppl):abstract 2503.
5. Adjei AA, Cohen RB, Franklin W, et al. Phase I pharmacokinetic and pharmacodynamic study of the oral, small-molecule mitogen-activated protein kinase kinase 1/2 inhibitor AZD6244 (ARRY-142886) in patients with advanced cancers. *J Clin Oncol*. 2008;26(13):2139–2146.
6. Gray-Schopfer VC, Karasarides M, Hayward R, Marais R. Tumor necrosis factor-alpha blocks apoptosis in melanoma cells when BRAF signaling is inhibited. *Cancer Res*. 2007;67(1):122–129.
7. VanBrocklin MW, Verhaegen M, Soengas MS, Holmen SL. Mitogen-activated protein kinase inhibition induces translocation of Bmf to promote apoptosis in melanoma. *Cancer Res*. 2009;69(5):1985–1994.
8. Eisenmann KM, VanBrocklin MW, Staffend NA, Kitchen SM, Koo HM. Mitogen-activated protein kinase pathway-dependent tumor-specific survival signaling in melanoma cells through inactivation of the proapoptotic protein bad. *Cancer Res*. 2003;63(23):8330–8337.
9. Davies BR, Logie A, McKay JS, et al. AZD6244 (ARRY-142886), a potent inhibitor of mitogen-activated protein kinase/extracellular signal-regulated kinase kinase 1/2 kinases: mechanism of action in vivo, pharmacokinetic/pharmacodynamic relationship, and potential for combination in preclinical models. *Mol Cancer Ther*. 2007;6(8):2209–2219.
10. Gopal YN, Deng W, Woodman SE, et al. Basal and treatment-induced activation of AKT mediates resistance to cell death by AZD6244 (ARRY-142886) in BRAF-mutant human cutaneous melanoma cells. *Cancer Res*. 2010;70(21):8736–8747.
11. Emery CM, Vijayendran KG, Zipser MC, Sawyer AM, Niu L, Kim JJ, et al. MEK1 mutations confer resistance to MEK and B-RAF inhibition. *Proc Natl Acad Sci U S A*. 2009;106(48):20411–20416.
12. Wagle N, Emery C, Berger MF, et al. Dissecting therapeutic resistance to RAF inhibition in melanoma by tumor genomic profiling. *J Clin Oncol*. 2011; 29(22):3085–3096.
13. Corcoran RB, Dias-Santagata D, Bergethon K, Iafrate AJ, Settleman J, Engelman JA. BRAF gene amplification can promote acquired resistance to MEK inhibitors in cancer cells harboring the BRAF V600E mutation. *Sci Signal*. 2010;3(149):ra84.
14. Johannessen CM, Boehm JS, Kim SY, et al. COT drives resistance to RAF inhibition through MAP kinase pathway reactivation. *Nature*. 2010;468(7326):968–972.
15. Nazarian R, Shi H, Wang Q, et al. Melanomas acquire resistance to B-RAF(V600E) inhibition by RTK or N-RAS upregulation. *Nature*. 2010;468(7326):973–977.
16. Villanueva J, Vultur A, Lee JT, et al. Acquired resistance to BRAF inhibitors mediated by a RAF kinase switch in melanoma can be overcome by cotargeting MEK and IGF-1R/PI3K. *Cancer Cell*. 2010;18(6):683–695.
17. Liu P, Cheng H, Roberts TM, Zhao JJ. Targeting the phosphoinositide 3-kinase pathway in cancer. *Nat Rev Drug Discov*. 2009;8(8):627–644.
18. Pal SK, Reckamp K, Yu H, Figlin RA. Akt inhibitors in clinical development for the treatment of cancer. *Expert Opin Investig Drugs*. 2010;19(11):1355–1366.
19. Balch CM, Gershenwald JE, Soong SJ, et al. Final version of 2009 AJCC melanoma staging and classification. *J Clin Oncol*. 2009;27(36):6199–6206.
20. Workman P, Aboagye EO, Balkwill F, et al. Guidelines for the welfare and use of animals in cancer research. *Br J Cancer*. 2010;102(11):1555–1577.
21. Levy C, Khaled M, Fisher DE. MITF: master regulator of melanocyte development and melanoma oncogene. *Trends Mol Med*. 2006;12(9):406–414.
22. Arozarena I, Bischof H, Gilby D, Belloni B, Dummer R, Wellbrock C. In melanoma, beta-catenin is a suppressor of invasion. *Oncogene*. 2011;30(45):4531–4543.
23. Wellbrock C, Marais R. Elevated expression of MITF counteracts B-RAF-stimulated melanocyte and melanoma cell proliferation. *J Cell Biol*. 2005;170(5):703–708.
24. Wellbrock C, Weisser C, Geissinger E, Troppmair J, Schartl M. Activation of p59(Fyn) leads to melanocyte dedifferentiation by influencing MKP-1-regulated mitogen-activated protein kinase signaling. *J Biol Chem*. 2002;277(8):6443–6454.
25. Kubic JD, Young KP, Plummer RS, Ludvik AE, Lang D. Pigmentation PAX-ways: the role of Pax3 in melanogenesis, melanocyte stem cell maintenance, and disease. *Pigment Cell Melanoma Res*. 2008;21(6):627–645.
26. Yang G, Li Y, Nishimura EK, et al. Inhibition of PAX3 by TGF-beta modulates melanocyte viability. *Mol Cell*. 2008;32(4):554–563.
27. Inoue Y, Imamura T. Regulation of TGF-beta family signaling by E3 ubiquitin ligases. *Cancer Sci*. 2008;99(11):2107–2112.
28. Tang LY, Yamashita M, Coussens NP, et al. Ablation of Smurf2 reveals an inhibition in TGF-beta signalling through multiple mono-ubiquitination of Smad3. *EMBO J*. 2011;30(23):4777–4789.
29. Hoek KS, Schlegel NC, Brafford P, et al. Metastatic potential of melanomas defined by specific gene expression profiles with no BRAF signature. *Pigment Cell Res*. 2006;19(4):290–302.
30. Massague J. TGFbeta in Cancer. *Cell*. 2008;134(2):215–230.
31. Haass NK, Sproesser K, Nguyen TK, et al. The mitogen-activated protein/extracellular signal-regulated kinase kinase inhibitor AZD6244 (ARRY-142886) induces growth arrest in melanoma cells and tumor regression when combined with docetaxel. *Clin Cancer Res*. 2008;14(1):230–239.
32. Denton CL, Gustafson DL. Pharmacokinetics and pharmacodynamics of AZD6244 (ARRY-142886) in tumor-bearing nude mice. *Cancer Chemother Pharmacol*. 2011;67(2):349–360.
33. Cragg MS, Jansen ES, Cook M, Harris C, Strasser A, Scott CL. Treatment of B-RAF mutant human tumor cells with a MEK inhibitor requires Bim and is enhanced by a BH3 mimetic. *J Clin Invest*. 2008;118(11):3651–3659.
34. Garraway LA, Widlund HR, Rubin MA, et al. Integrative genomic analyses identify MITF as a lineage survival oncogene amplified in malignant melanoma. *Nature*. 2005;436(7047):117–122.
35. Dynek JN, Chan SM, Liu J, Zha J, Fairbrother WJ, Vucic D. Microphthalmia-associated transcription factor is a critical transcriptional regulator of melanoma inhibitor of apoptosis in melanomas. *Cancer Res*. 2008;68(9):3124–3132.
36. McGill GG, Horstmann M, Widlund HR, et al. Bcl2 regulation by the melanocyte master regulator Mitf modulates lineage survival and melanoma cell viability. *Cell*. 2002;109(6):707–718.
37. Wellbrock C, Rana S, Paterson H, Pickersgill H, Brummelkamp T, Marais R. Oncogenic BRAF regulates melanoma proliferation through the lineage specific factor MITF. *PLoS One*. 2008;3(7):e2734.

38. Blank M, Tang Y, Yamashita M, Burkett SS, Cheng SY, Zhang YE. A tumor suppressor function of Smurf2 associated with controlling chromatin landscape and genome stability through RNF20. *Nat Med*. 2012;18(2):227–234.
39. Ramkumar C, Kong Y, Cui H, et al. Smurf2 regulates the senescence response and suppresses tumorigenesis in mice. *Cancer Res*. 2012;72(11):2714–2719.
40. Narimatsu M, Bose R, Pye M, et al. Regulation of planar cell polarity by Smurf ubiquitin ligases. *Cell*. 2009;137(2):295–307.
41. Fukunaga E, Inoue Y, Komiya S, et al. Smurf2 induces ubiquitin-dependent degradation of Smurf1 to prevent migration of breast cancer cells. *J Biol Chem*. 2008;283(51):35660–35667.
42. Jin C, Yang YA, Anver MR, Morris N, Wang X, Zhang YE. Smad ubiquitination regulatory factor 2 promotes metastasis of breast cancer cells by enhancing migration and invasiveness. *Cancer Res*. 2009;69(3):735–740.
43. Zhang H, Cohen SN. Smurf2 up-regulation activates telomere-dependent senescence. *Genes Dev*. 2004;18(24):3028–3040.
44. Fukuchi M, Fukai Y, Masuda N, et al. High-level expression of the Smad ubiquitin ligase Smurf2 correlates with poor prognosis in patients with esophageal squamous cell carcinoma. *Cancer Res*. 2002;62(24):7162–7165.
45. Eichhorn PJ, Rodon L, Gonzalez-Junca A, et al. USP15 stabilizes TGF-beta receptor I and promotes oncogenesis through the activation of TGF-beta signaling in glioblastoma. *Nat Med*. 2012;18(3):429–435.
46. Hatzivassiliou G, Song K, Yen I, et al. RAF inhibitors prime wild-type RAF to activate the MAPK pathway and enhance growth. *Nature*. 2010;464(7287):431–435.
47. Heidorn SJ, Milagre C, Whittaker S, et al. Kinase-dead BRAF and oncogenic RAS cooperate to drive tumor progression through CRAF. *Cell*. 2010;140(2):209–221.
48. Cohen P, Tcherpakov M. Will the ubiquitin system furnish as many drug targets as protein kinases? *Cell*. 2010;143(5):686–693.

Funding

This work was supported by Cancer Research UK (C11591/A10202 and C11876/A12724). MS is funded by the BBSRC (FA01472 FLS) and the Alumni Fund of the Manchester University.

Notes

The sponsors of this study had no role in the collection of the data, the analysis and interpretation of the data, the decision to submit the manuscript for publication, or the writing or the manuscript.

Affiliations of authors: Molecular Cancer Studies, Wellcome Trust Centre for Cell Matrix Research, University of Manchester, Manchester, UK (MS, JF, IA, AC, AH, CW); Division of Cancer Biology, The Institute of Cancer Research, Chester Beatty Laboratories, London, UK (RH, RM).